PHILOSOPHICAL TRANSACTIONS OF THE ROYAL SOCIETY A MATHEMATICAL, PHYSICAL & ENGINEERING SCIENCES

Optimization and Modelling of Fuel Cell Electrodes with Emphasis upon Catalyst Utilization Ageing Phenomena and Ageing Prevention [and Discussion]

Hartmut Wendt, Thomas Brenscheidt, Andreas Fischer and K. Kendall

Phil. Trans. R. Soc. Lond. A 1996 **354**, 1627-1641
doi: 10.1098/rsta.1996.0069

Optimization and modelling of fuel cell electrodes with emphasis upon catalyst utilization ageing phenomena and ageing prevention

By Hartmut Wendt, Thomas Brenscheidt and Andreas Fischer

Institut für Chemische Technologie, TH Darmstadt Petersenstraße 20, D-64287 Darmstadt, Germany

Fuel cell electrodes demand specifically designed electrode structures and electrocatalyst morphologies. Low-temperature cell electrodes are composed of highly dispersed carbon, on the inner surface of which the catalyst, i.e. platinum or platinum alloys, is distributed as nanocrystals. Pt catalyst particles are most effectively stabilized by using Pt alloys. These catalysts together with dispersed PTFE are worked in electrodes into submicron scale agglomerates establishing micron pores between the agglomerates, kept open for fast diffusive gas transport. Agglomerates and the hydrophilic part of the pores are flooded by the electrolyte. In high-temperature cells typical structural features are established on a micron scale. Nickel sinter anodes in MCFCs and SOFCs are most effectively stabilized by dispersion hardening. Modelling of the different electrode structures allows us to understand mass transfer and conductivity limitations of fuel cells and helps to improve catalyst utilization and cell performance.

1. Introduction

Today five fuel cell technologies are known, all working on hydrogen as the fuel and oxygen or air as the oxidant. The direct methanol combusting fuel cell is an exception from this rule.

The low-temperature cells are:

(i) the alkaline fuel cell (AFC), working below 100 °C with 30 wt% KOH as electrolyte ($T \approx 100$ °C);

(ii) the phosphoric acid fuel cell (PAFC), working at approximately 200 °C with concentrated (103 wt%) phosphoric acid ($T \approx 180$–200 °C);

(iii) the proton-exchange membrane fuel cell (PEMFC) with a water-swollen perfluorinated sulphonic acid ionomer as electrolyte. This cell is used with a particularly modified electrocatalyst for direct methanol combusting cells (DMFC) ($T \approx 80$–130 °C).

Two high-temperature fuel cell technologies exist:

(i) The molten carbonate fuel cell (MCFC), which most frequently uses a eutectic melt containing 38/62 mole/mole% potassium and lithium carbonate and less frequently 48/52 mole/mole%, lithium and sodium carbonate ($T \approx 650$–700 °C).

Phil. Trans. R. Soc. Lond. A (1996) **354**, 1627–1641
Printed in Great Britain

(ii) Solid oxide fuel cells (SOFC) which use oxygen anion conducting yttria stabilized zirconia (YSZ) as the electrolyte ($T \approx 900$–$1000\,^{\circ}\mathrm{C}$).

Only the PAFC technology has become so mature that it is beginning to compete in the marketplace within the sector of medium-sized methane-fired cogeneration plants (several 100 kW) with conventional diesel-based units. MCFCs are developed to the extent of allowing a 2 MW demonstration plant to run in Santa Clara, CA, over the next few years.

2. Electrocatalysis of anodic hydrogen oxidation and cathodic oxygen reduction and the chemical nature of electrocatalysts

(a) *Anodic hydrogen oxidation*

The anode reaction, equation (2.1), is the conversion of hydrogen into protons and electrons producing in acid fuel cells solvated protons at the anode:

$$\mathrm{H_2} \rightarrow 2\mathrm{H^+} + 2\mathrm{e^-}. \tag{2.1}$$

This reaction may be modified according to the nature of the electrolyte, e.g. in alkaline molten carbonate and solid oxide cells by participation of oxygen anions ($\mathrm{O^{2-}}$) or oxygen anion carriers ($\mathrm{OH^-}$ or $\mathrm{CO_3^{2-}}$, respectively) so that in these cells the proton combines with $\mathrm{O^{2-}}$, $\mathrm{OH^-}$ or $\mathrm{CO_3^{2-}}$ to form water or water vapour in AFCs or water vapour and carbon dioxide from $\mathrm{CO_3^{2-}}$ in MCFCs.

Methane, and in the future also coal gas, is the primary fuel. Since $\mathrm{CH_4}$ as well as carbon monoxide react slowly at the anode, all fuel cells need chemical conversion of these fuels into hydrogen by steam reforming (equation (2.2)) and shift conversion (equation (2.3)),

$$\mathrm{CH_4} + \mathrm{H_2O} \rightarrow \mathrm{CO} + 3\mathrm{H_2}, \tag{2.2}$$

$$\mathrm{CO} + \mathrm{H_2O} \rightarrow \mathrm{CO_2} + \mathrm{H_2}, \tag{2.3}$$

either in external reactors (external reforming) or in the cell, which then either houses additionally the chemical catalyst, e.g. in MCFCs, or whose electrode acts simultaneously as an electrocatalyst and chemical catalyst as in SOFCs (internal reforming).

Reaction (2.1) is catalysed by all metals which are known to catalyse the splitting of dihydrogen, equation (2.4), by chemisorption

$$\mathrm{H_2} \rightleftharpoons 2\mathrm{H_{ad}}. \tag{2.4}$$

These are all platinum metals, with Pt being the most active and the transition metals iron, cobalt and nickel. Ni is seven to ten times more expensive than iron (Wendt 1988), which, however, is unsuitable because it is less noble than hydrogen and would not persist in $\mathrm{H_2/H_2O}$ mixtures. The theoretical background of the catalytic and electrocatalytic properties of different metals is the electronic structure of the respective bulk material and of the surface atoms exposed to the gas phase or the electrolyte, respectively (Ristic *et al.* 1995). These properties are expressed in the well known vulcano curves (Trasatti 1972).

(b) *Cathodic oxygen reduction*

Electrocatalysed reduction of dioyxgen to divalent oxygen anions, equation (2.5 *a*), proceeds at fuel cell cathodes always in the adsorbed states,

$$\mathrm{O_2} + 4\mathrm{e^-} \rightarrow 2\mathrm{O^{2-}} \quad \text{(at SOFC cathodes)}. \tag{2.5\,a}$$

PHILOSOPHICAL TRANSACTIONS OF THE ROYAL SOCIETY A MATHEMATICAL, PHYSICAL & ENGINEERING SCIENCES

This four-electron reaction is more complex than anodic hydrogen oxidation. The reaction is therefore more hindered and kinetically more demanding and overpotentials are higher. According to the nature of the electrolyte the total reaction is modified.

In acidic electrolytes water or water vapour is formed at the cathode,

$$O_2 + 4e^- + 4H^+ \rightarrow 2H_2O, \tag{2.5\,b}$$

and in alkaline electrolytes hydroxyl anions are produced,

$$O_2 + 4e^- + 2H_2O \rightarrow 4OH^-, \tag{2.6}$$

whereas O^{2-} reduction in carbonate melts demands the presence of carbon dioxide,

$$O_2 + 4e^- + 2CO_2 \rightarrow 2CO_3^{2-}. \tag{2.7}$$

Without going into the details of the mechanism, in protic solvents the total reaction proceeds in two or more kinetically distinct steps.

Four-electron reductions are scarce and of little practical relevance (with aza-complexes of Co(II)-ions as electrocatalysts (Collmann *et al.* 1980; Durant *et al.* 1983), and at Tl-modified gold electrodes (Mc Intyre & Peck 1980; Collmann *et al.* 1979).

The standard potential for hydrogen peroxide generation—an intermediate—is 700 mV more negative than that for cathodic water formation. Therefore fast removal of H_2O_2 is imperative in order to reduce substantially the cathodic overvoltage. It is obvious that any metal or electronically conducting or semiconducting metal oxide which catalyses hydrogen peroxide disproportionation might be a good electrocatalyst for cathodic oxygen reduction.

In aqueous alkaline solutions transition metal oxides which may undergo a change of oxidation state (e.g. Mn(II)/Mn(III), Fe(II)/Fe(III) or Co(II)/(III)), for example, $NiCo_2O_4$, $LaMnO_3$ or $LaNiO_3$ and La, Sr, Ni, Co-perovskites (Kirchnerova *et al.* 1995) have been examined as cathodic catalysts. However, their long-term stability is questioned. The role of platinum as the catalyst of choice for oxygen reduction in low-temperature cells is unique and rests on the catalytic properties of the bare platinum metal surface. Under practical conditions the cathodic overpotential is kept sufficiently high to prevent the platinum surface from becoming oxidized and covered by a PtO layer. In spite of the high price of this metal its catalytic activity is so high, and its utilization can be enhanced to such an extent, that there does not exist any alternative for platinum for low-temperature cells.

In high-temperature cells the cathodes are p-type semiconducting oxides, the catalytic activity of which is likely to be due to redox reactions at their surface. In molten carbonate fuel cells it is lithiated nickel oxide containing from 1 to 2 mole% lithium oxide with an electronic conductivity of the order of 10 S cm^{-1}. $LiCoO_2$ is under discussion as an alternative cathode material (Kucera *et al.* 1993; Appleby & Foulkes 1988).

For solid oxide fuel cells, the material most used today is Sr-doped $LaMnO_3$ (Plomp & Huijsmann 1995) but lanthanum cobaltite, $LaCoO_3$, is also reported.

In MCFCs, oxygen reacts with the electrolyte and dissolves in the form of peroxy-anions:

$$O_2 + 2CO_3^{2-} \rightarrow 2O_2^{2-} + 2CO_2, \tag{2.8}$$

the reduction of which to O^{2-} or CO_3^{2-} is fast, so that the transport of these oxygen species from the electrolyte–gas interface to the surface of the NiO crystals, which constitutes the cathode, becomes rate determining.

3. Structure of gas diffusion electrodes—the so-called three-phase boundary

Gas diffusion electrodes are porous and composed of corrugated electrode material with relatively wide, gas-conducting pores which allow for easy access of working gases to the inner surface of the electrode. Penetration of the electrolyte into this structure and filming and wetting of the inner surface is indispensible. Internal wetting of the porous electrode together with the existence of non-flooded open gas-conducting pores creates the so-called three-phase boundary, which is essentially constituted by the formation of thin layers and menisci of electrolyte on the internal surface of the electrode.

4. Particle size and catalyst utilization

In order to utilize the electrode metal or oxidic material to the highest possible extent, it is to be subdivided as finely as possible as the mass-related surface $S = A/m$ of any particle increases with the inverse of the particle's extension d:

$$\frac{A}{m} = S = \frac{f}{d\rho}, \tag{4.1}$$

where f is the numerical value of the surface-to-volume ratio and ρ is the density.

It is not possible to subdivide the catalyst particle to any desired degree. A material becomes less stable the finer its granularity becomes, because of the increasing excess molar surface Gibbs energy $\Delta\mu$ (surface), which is calculated in equation (4.2),

$$\Delta\mu(\text{surface}) = SM\sigma = \frac{Mf\sigma}{d\rho}, \tag{4.2}$$

(where M is the molecular weight and σ is the surface tension of the dispersed material). As finely dispersed materials tend to aggregate, by Ostwald ripening due to dissolution–deposition, Brownian motion or other thermally activated processes, the operating temperature of the cell determines the degree of dispersion to which catalyst particles are virtually stable.

Metallic catalysts such as platinum or nickel dispersed to nanometre size, are still stable in low-temperature cells operating below 200 °C. Therefore Raney nickel, a highly porous sponge-like nickel material with pore diameters of 2–3 nm, is a typical anodic electrocatalyst used in the early days for alkaline fuel cells. The pores in Raney nickel are not supposed to be cylindrical but the sponge-like structure resembles more that of a grid and ashbar morphology. Generally, the cylindrical pore is not a suitable model. Nanoparticles of platinum on nanostructured active carbon or soot for cathodes and anodes of AFCs, PAFCs and PEMFCs are today's state of the art. The micrograph of figure 1 gives an impression of how Pt particles are distributed on active carbon. The active carbon come in agglomerates and flakes of 0.1–0.3 μm diameter. As pointed out by Kinoshita (Kinoshita & Stonehart 1988; Kinoshita 1992), for Pt particles the mass-related catalytic activity passes through a maximum at a crystal size of 2–4 nm. It makes little sense to decrease the particle size below 1 or 2 nm. At a crystallite dimension of 2 nm approximately 30% of the atoms contained in the crystal are surface atoms.

In MCFCs (650–700 °C) and SOFCs (900–1000 °C) nanoporosity or nanogranulometry of metals is lost in fractions of an hour by sintering and compaction. Relatively

Figure 1. Transmission electron micrograph of Pt-activated carbon.

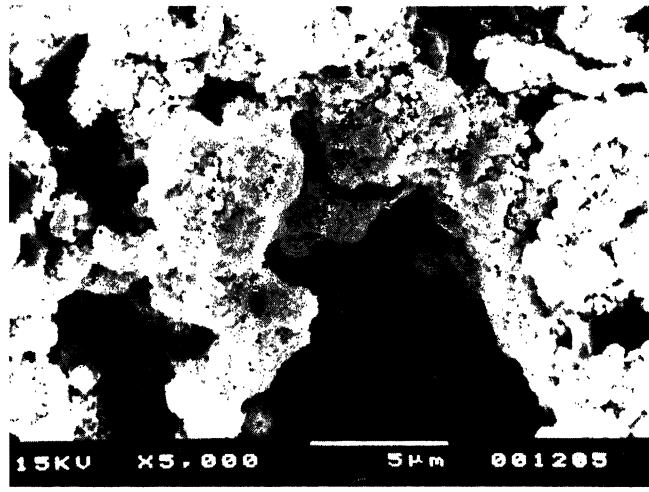

Figure 2. Scanning electron micrograph of a NiO cathode for MCFC.

stable—on a several hundred hours basis—become transition metal micron-sized particles, the typical size of granules of the nickel sinter used for MCFC anodes. But still particular measures have to be taken to stabilize them in order to obtain morphological stability over 40 000 h.

The conventional cathodes of MCFC are composed of lithiated agglomerates of tiny submicron crystals of NiO (figure 2). The agglomerates are composed of hundreds of these crystallites as they are formed *in situ* from a nickel-sinter precursor by chemical oxidation with air. Also the tiny NiO particles have a tendency to grow, but rather by dissolution–deposition than by sintering.

5. Bimodal pore size distribution of gas diffusion electrodes with liquid electrolyte

The porous catalyst proper has to be soaked with electrolyte in order to contact ionically the whole catalyst surface. As important as the ionic contact to the catalyst surface is the supply of the working gas (fuel or oxidant) to the outer wetted surface of the electrocatalyst particle or agglomerate by open gas-conducting pores.

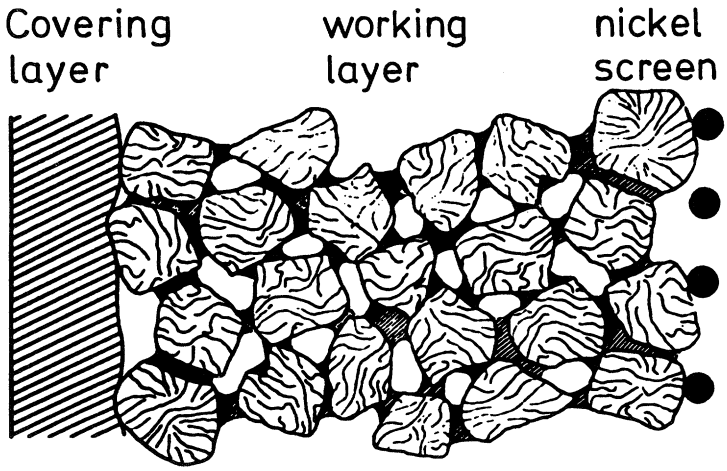

Figure 3. Schematic cross section—not drawn to scale with respect to catalyst particles—of a Raney-nickel anode.

Figure 3 depicts schematically the structure of a Raney-nickel anode of an AFC of approximately 0.5 mm thickness with wide (20–50 μm) non-flooded gas pores, constituting 20–30% of the volume of the electrode between the nanoporous Raney-nickel catalyst (Mund *et al.* 1977). The flooded catalyst ($dp \approx 5$–$10\,\mu m$) has 20–30 vol% porosity with pores of approximately 2 nm. Similarly, the coarser nickel oxide cathode of the MCFC depicted in figure 2 is composed of wide gas conducting pores with 3–5 μm pore radius occupying approximately 20–30% of the cathode volume and supplying the 3–6 μm agglomerates of very small (*ca.* 0.1 μm) NiO crystals (20% porosity) with oxygen.

PTFE-bonded Pt-activated soots are used for over 20 years for PAFC anodes and cathodes. Their structure is similar to that of PTFE-bonded Raney nickel—only that catalyst agglomerates come in sizes of fractions of micrometres rather than several micrometres. They also have a bimodal pore structure and it was believed that the gas-conducting pores are kept free of electrolyte by a hydrophobic film of PTFE. However, Murakashi and colleagues showed recently that this is not true. Over a long time the PTFE is converted and degraded chemically and loses its hydrophobic properties (Aragane *et al.* 1994).

In all these electrodes with bimodal pore size distributions it is the principle of the equilibrium of capillary forces in a porous matrix and the total amount of electrolyte available in the electrode which determines the distribution of the liquid electrolyte between pores of different diameter.

According to the Young–Laplace equation

$$\Delta p = \frac{\sigma \cos\theta}{d}, \tag{5.1}$$

where θ is the wetting angle and σ is the surface tension of the electrolyte, an overpressure Δp must be exerted to push the electrolyte with the surface tension at the electrolyte–gas interface which wets the catalyst material with the wetting angle θ out of a pore with diameter d. If there is only a limited supply of electrolyte then all the finest pores are completely filled and the coarser ones are only filled to the degree to which the electrolyte supply would allow.

PHILOSOPHICAL TRANSACTIONS OF THE ROYAL SOCIETY A MATHEMATICAL, PHYSICAL & ENGINEERING SCIENCES

6. Electrode structures of fuel cells with solid electrolytes

PEMFCs and SOFCs are comparable insofar as the electrolyte is not a fluid. It is a quasi-solid proton-conducting ionomer on one hand and a true solid, the partial ionic sublattice of which is almost liquid on the other hand.

The electrocatalyst of PEMFCs, Pt-activated carbon, which is completely soaked with the ionomer, forms a very thin layer on the ionomeric membrane. The electrodes are 5–10 μm thick, have a porosity of 5–30% and are firmly glued to the membrane. The membrane with a thickness of between 50 and 150 μm is much thicker than the electrodes.

A typical SOFC is composed of a 75–100 μm thick zirconia membrane, a relatively thick (*ca.* 100 μm) porous cathode and a porous Ni–ZrO_2 cermet anode which is only 10 μm thick. The details of this cell will be dealt with in Steele (this volume).

7. Ageing of fuel cell electrodes and ageing prevention

(*a*) *Reversible and irreversible catalyst deterioration*

Ageing and deterioration of electrocatalysts is as usual as that of chemical catalysts. One should distinguish deterioration by poisoning, which most often is a reversible effect, from deterioration accomplished by slowly changing morpohlogy—the ageing effect proper, which is completely irreversible. Gas diffusion electrodes of low- and high-temperature cells demand specifically different means to prevent or decelerate ageing.

(*b*) *Ageing and ageing prevention in low-temperature cells*

Already in the late 1960s (Mund *et al.* 1977) it was realized that Raney nickel used as an electrocatalyst deteriorates over a timescale of 1000 to several 1000 h as the material loses its catalytic activity due to loss of catalyst surface by recrystallization.

Addition of some Ti to the precursor alloy of Raney nickel (Ni_2Al_3 and $NiAl_3$) improves the longevity because TiO_2 precipitates in the microporous structure slowing down the recrystallization of the nanoporous material by dispersion hardening.

Several ageing processes are discussed for Pt-activated carbon, which today is the catalyst of choice for AFCs, PAFCs and PEMFC:

(i) Anodic dissolution of Pt in the form of Pt(II), its diffusion towards the anode and plating out at the anode.

(ii) Agglomeration of particles by encounter due to stochastic Brownian motion on the soot particle.

(iii) Anodic oxidation of the support.

Mechanisms (i)–(iii) are observed at the oxygen cathode which ages faster than the anode. Mechanism (i) is a serious cause of Pt losses and catalyst deterioration. It is potential dependent and accelerates under partial load or in off-time when the cathode potential drifts towards the oxygen equilibrium potential. It is therefore usual to keep the load always sufficiently high to prevent the cathode potential from drifting above −200 mV versus the oxygen equilibrium potential, the threshold for PtO formation. Whenever the fuel cell is switched off, the oxygen in the cathode lumen is rapidly exchanged for inert nitrogen and the cathode is put at the anode potential.

Deterioration by agglomeration, mechanism (ii), is successfully mitigated by using Pt alloys withstanding mechanisms (i) and (ii), which are applied in a comparable degree of dispersion but somewhat coarser than pure Pt.

PHILOSOPHICAL TRANSACTIONS OF THE ROYAL SOCIETY A MATHEMATICAL, PHYSICAL & ENGINEERING SCIENCES

By reaction of dispersed Pt on soot with non-noble metals of group VI B and V B, dispersed alloys are formed (Bett 1992; Stonehart 1990; Ito *et al.* 1988; Itoh & Katoh 1990; Jalan 1979, 1985; Kush 1988). Treating Pt-impregnated carbon, to which salts of these metals had been added, at 900 °C in an inert atmosphere (Ar) leads, for example, to formation of highly dispersed Pt–Cr or Pt–V alloys. The alloy crystallites are reported to be highly active cathode catalysts for PAFCs. But they dissolve quickly in concentrated phosphoric acid. Tertiary and also quarternary alloys containing transition metals of group VIII are much more stable than the binary alloys and additionally show a higher catalytic activity than platinum alone. Ternary alloy catalysts with Pt–Co–Cr are reported to be the most active ones (Fuller *et al.* 1995), and would stand a lifetime of 40 000 h. The observed enhancement of the catalytic activity of these Pt alloys is not understood—neither is their stability in concentrated phosphoric acid at 200 °C.

Yeager and co-workers recently showed that the nickel–platinum bronze $Ni_xPt_3O_4$ is an excellent and stable O-reduction catalyst in H_3PO_4 (Tryk *et al.* 1994). It is not unlikely that from Pt alloys such bronzes are formed *in situ* constituting the catalyst proper. At PAFC anodes, alloy catalysts of Pt and Pd are used. The mixed catalyst is cheaper and more active than Pt (Stonehart 1990). Alloying of Pt with Pd has allowed a reduction of anode catalyst loading to 0.1 mg cm^{-2}.

Carbon is unstable at the cathode due to the corrosion reaction

$$C + H_2O \leftrightarrow CO + 2H^+ + 2e^-. \tag{7.1}$$

At the cathode the carbon support of the Pt catalyst is anodically oxidized (Scholta 1993). Heating active carbons to 2000 °C leads to graphitization of these materials. Thereby the specific surface decreases from typically 100–150 $m^2\ g^{-1}$ to only 50 $m^2\ g^{-1}$—in this aspect the heat treatment is detrimental. But the corrosion rate is slowed down by orders of magnitudes. Still the graphitized material corrodes anodically at the cathode potential, so that after a lifetime of 40 000 h only one third of the initially present carbon is still there.

(*c*) *Ageing and its retardation in high-temperature cells*

(i) MCFC

The anodes of molten carbonate cells are made of a nickel sinter, the internal structure of which is depicted in figure 4. It is known that creep and progressive plastic deformation accompanying sintering lead to fast deterioration of the anode but can be retarded by dispersion hardening (Exner 1978) which can be brought about, for example, by internal oxidation of alloys (Rhines 1940) containing non-noble metals such as, for example, aluminium or chromium. For this reason it is the state of the art to use alloys, for instance Ni15Cr or Ni15Al instead of pure nickel. The alloys are much harder, their Brinell hardness is approximately a factor of 6 higher than that of pure Ni, this retards anode creep and compaction considerably. But the more important long-term effect is due to slow oxidation of Cr and Al which diffuse to the internal surface of the sinter and are oxidized there forming sparcely soluble salts with the electrolyte—equation (7.2),

$$2Cr(Al) + 3Li_2CO_3 \rightarrow 2LiCrO_2(LiAlO_2) + 2Li_2O + 3CO, \tag{7.2}$$

which give rise to external dispersion hardening. The same effect is achieved if an externally hardening agent, e.g. Li_2TiO_3, is added to pure nickel before preparing the sinter as depicted in figure 4 (Böhme *et al.* 1994).

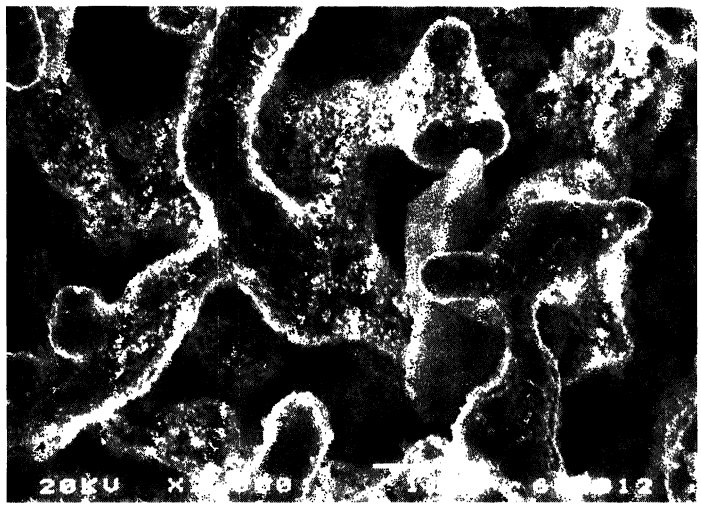

Figure 4. Scanning electrode micrograph of Li_2TiO_3-stabilized sintered nickel anode (MCFC).

Lithiated nickel oxide cathodes are prepared in the cell by atmospheric oxidation of sintered nickel in contact with the electrolyte at 600–650 °C. It is well known (Ota *et al.* 1992) that the solubility of this material, approximately 30 wt ppM, is too high as it gives rise to serious life limitations. The solubility due to the reaction

$$NiO + CO_2 \rightarrow Ni^{2+} + CO_3^{2-}, \tag{7.3}$$

is sufficiently high to make the mass transfer velocity for this ion towards the anode, which is a sink for nickel ions, too fast. Short circuiting of the cell by nickel dendrites, spreading from the anode endangers cell performance and cell life already after 1000 h of operation (Kunz 1991). This problem has not really been solved. There are two ways to mitigate cathode dissolution: either finding means to decrease the solubility of nickel oxide in the electrolyte or finding an alternative electrode material with substantially lower solubility. By changing the electrolyte composition from 62%/38% Li_2CO_3/K_2CO_3 to 50%/50% Li_2CO_3/Na_2CO_3 the solubility of NiO drops, but only by a factor of 3. Adding alkali earth carbonates, such as $CaCO_3$ or $BaCO_3$, to alkali carbonate melts also affects the solubility of NiO in the same sense (Doyon *et al.* 1987), so that an overall decrease of solubility and mass transfer rate of the cathode material of a factor of ten can be expected in combining the Li–Na electrolyte with added alkaline earth carbonates.

The second option would be to use $LiCoO_2$ a remarkably more expensive material than NiO—as the cathode material because its solubility is a factor of ten lower than that of nickel oxide. This material being also a p-type semiconductor has too low electronic conductivity, approaching only 1 S cm^{-1} under operating conditions (Brown *et al.* 1992; Kudo *et al.* 1995). Therefore particular current collecting structures would have to be applied to support porous $LiCoO_2$ cathodes.

(ii) SOFC

Since all components of the cell are solid in SOFCs and the metallic nickel anode is morphologically stabilized by being a component of a cermet there is relatively little concern about long-term morphological changes in this cell. As will be dealt with in the contribution by Steele in this volume, it is more the chemical reaction

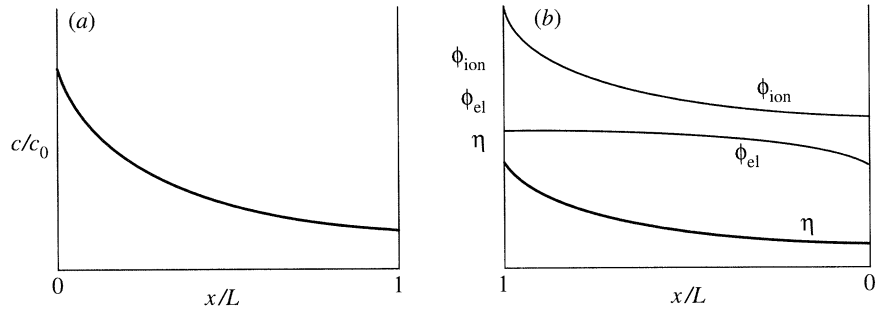

Figure 5. Schematic presentation of (*a*) concentration decay (of H_2 or O_2) and (*b*) of overpotential with increasing distance from (*a*) gas phase side of and (*b*) electrolyte side of a gas diffusion electrode.

of, for example, the alkaline earth components in the cathode with the zirconia membrane which deteriorates the cell. The ongoing yearly conferences on SOFCs and SOFC materials testify that there exist a host of as yet unsolved problems.

8. Modelling of fuel cell electrodes and fuel cells

(*a*) *Purpose of modelling*

The factors which influence the performance of electrodes and cells are numerous, such as mass transport of the reactants in gas-conducting pores and electrolyte-flooded catalyst particles, agglomerates or sheets, electric conductivity of the electrode matrix and the electrolyte, the effective cell potential applied and heat generation due to the electrochemical reaction. Their interaction gives rise to current density distributions within catalyst particles, agglomerates and the electrode depth and also along the flow direction of the gases. This eventually determines the measurable current–voltage relation of the cell. It is the purpose of modelling to identify the most important factors affecting fuel cell performance and to help to improve the morphology and other relevant physical properties of electrodes in order to improve cell performance, catalyst utilization and reduce electricity costs.

If physically discernable catalyst particles or their agglomerates are small compared to the electrode thickness, such as for instance in Raney-nickel anodes according to Mund (Mund *et al.* 1977; Mund & Sturm 1975) the first step in modelling concentrates on calculating reactant concentration profiles (figure 5*a*) in catalyst particles and to determine from the depletion of the reactant the degree of utilization of the catalyst at a given overpotential, neglecting any potential changes within the electrode and electrolyte phase (Yang *et al.* 1990; Cutlip *et al.* 1991). The next step includes calculating the ohmic potential drops parallel to the electric current perpendicular to the electrode surface.

(*b*) *Dimensonless figures characterizing catalyst utilization*

The differential equations used to describe concentration profiles of depolarizers in porous catalyst particles on the one hand and the potential distribution in porous electrodes on the other hand allow us to define dimensionless quantities such as for instance the 'Thiele modulus', Φ_{Th}, which comprise several parameters, which define the system under discussion. This allows us to simplify the treatment considerably as the number of independent parameters is reduced and these dimensionless numbers are simultaneously figures of merit. If Φ_{Th}, exceeds a value of 3, catalyst utilizations

become low and approach Φ_{Th}^{-1}. If Φ_{Th} is smaller than 1 the utilization approaches unity (El-Anadouli *et al.* 1991). The Thiele modulus is given by $\Phi_{\mathrm{Th}} = d_{\mathrm{p}}(r_{\mathrm{v}}/c_0 D)^{1/2}$ with d_{p} the particle diameter, r_{v} the reaction rate per unit volume in the porous catalyst, c_0 the bulk concentration of the reactant and D its diffusion coefficient.

(*c*) *Concentration polarization in porous catalyst particles and agglomerates*

The differential equation describing competitive mass transfer and reaction of, for example, anodic oxidation of hydrogen in a flooded catalyst particles reads

$$D\nabla^2 c_{\mathrm{R}} = r_{\mathrm{v}}, \tag{8.1}$$

where D is the effective diffusion coefficient, c_{R} the reactant concentration, r_{V} the volume-specific reaction rate of the catalyst, given by the volume-specific catalyst surface A_{V}, and the surface specific reaction rate which for electrochemical reactions is determined by current densities. These are determined by the given overpotential and the ratio of the local concentration of the reactant c_{l} and its concentration at the inner surface of the catalyst particle c_0,

$$D\nabla^2 c_{\mathrm{R}} = A_{\mathrm{V}} \mathrm{i}(\eta, c_{\mathrm{l}}/c_0, x, y, z)/\nu_{\mathrm{e}} F, \tag{8.2}$$

where ν_e is the electrons' stoichiometry factor, e.g. 2 for H_2 oxidation and 4 for O_2 reduction. Concentration profiles and catalyst utilization of a single particle or small agglomerates can be expressed as a function of the dimensionless electrochemical Thiele modulus Φ_{Th} for spherical particles

$$c_{\mathrm{l}}/c_0 = f_{\mathrm{N}} \frac{\cosh \Phi_{\mathrm{Th}}(1 - x/d_{\mathrm{p}})}{\cosh \Phi_{\mathrm{Th}}}, \tag{8.3}$$

with f_{N} a numerical factor of value close to 1 and x the distance from the particle centre,

$$\text{cat. utiliz.} = I_{\text{effective}}/I_{\max} = \Phi_{\mathrm{Th}}^{-1} \tanh \Phi_{\mathrm{Th}}, \tag{8.4}$$

with the limit Φ^{-1} for $\Phi > 5$.

Formally, Φ_{Th} reads differently for the fast hydrogen oxidation, the rate of which according to the generalized Butler–Volmer equation has to consider forward and back reaction and the oxygen reduction where (at least in low-temperature cells) only the forward reaction has to be considered:

$$\Phi_{\mathrm{Th\ rev}} = d_{\mathrm{p}}(i_0(\alpha_a + \alpha_c)\eta A_{\mathrm{V}}/DRTc_0\nu_{\mathrm{e}})^{1/2}, \tag{8.5}$$

$$\Phi_{\mathrm{Th\ irrev}} = d_{\mathrm{p}}(i_0 A_{\mathrm{V}}/Dc_0 F\nu_{\mathrm{e}})^{1/2} \exp\{\alpha_c \eta/2b\} \quad \text{with } b = RT/F. \tag{8.6}$$

The faster the reaction is, the more the reactant is depleted in the catalyst and the lower the catalyst utilization is. A mass-transport-limited current density, which is very often observed is not predicted. Therefore the model is amended to include an electrolyte film covering the flooded particle or agglomerate (Yang *et al.* 1990; Cutlip 1991). Examples for low catalyst utilization or high Thiele modulus are Raney-nickel particles with $d_{\mathrm{p}} > 10\ \mu\mathrm{m}$ (Mund *et al.* 1977), the NiO agglomerates in MCFCs (Fontes *et al.* 1995) or too thick PAFC cathodes (Fuller *et al.* 1995).

(*d*) *Ohmic potential drop in the electrode*

Figure 5*b* shows an example for the spatial change of overpotential perpendicular to the electrode surface caused by the ohmic potential drop in the electrolyte and the electrode matrix. The one-dimensional change of the overpotential is given by

Ohm's law applying the local, formal current density i_l within the electrode. If the electrode (el) and electrolyte (ion) phase are assumed to be quasi-homogeneous one obtains

$$\frac{\mathrm{d}\varphi_{\mathrm{el}}}{\mathrm{d}x} = \rho_{\mathrm{el}} i_{\mathrm{el}}, \quad \frac{\mathrm{d}\varphi_{\mathrm{ion}}}{\mathrm{d}x} = \rho_{\mathrm{ion}} i_{\mathrm{ion}}, \tag{8.7}$$

taking into account $\mathrm{d}i_{\mathrm{el}} = -\mathrm{d}i_{\mathrm{ion}}$ and $\mathrm{d}(\varphi_{\mathrm{el}} - \varphi_{\mathrm{ion}}) = \mathrm{d}\eta$ results in

$$\frac{\mathrm{d}^2\eta}{\mathrm{d}x^2} = (\rho_{\mathrm{el}} + \rho_{\mathrm{ion}}) A_{\mathrm{V}} i(\eta, x). \tag{8.8}$$

For a hindered reaction, introducing the term of the forward reaction as an oxygen reduction for i only allows us to define another dimensionless term for exclusive ohmic and negligible mass transfer control,

$$\Phi_\Omega = H((\rho_{\mathrm{el}} + \rho_{\mathrm{ion}}) A_{\mathrm{V}} i_0 \alpha / 2b)^{1/2} \exp\{\eta\alpha/2b\}, \tag{8.9}$$

where H is the thickness or height of the electrode layer.

The resulting distribution of overpotential and local current density with negligible mass transport limitations is quite similar with respect to the electrode depth as it was with concentration and current density within a catalyst particle or agglomerate. For sufficiently high overpotentials (oxygen reduction) one obtains the macroscopic current density of the electrode as

$$i_{\mathrm{eff}} = (2 i_0 A_{\mathrm{V}} c_0 / (\rho_{\mathrm{el}} + \rho_{\mathrm{ion}}))^{1/2} \exp\{\eta\alpha/2b\}. \tag{8.10}$$

Note that this expression is independent of H and would have to be compared to a value of

$$i_{\max} = A_{\mathrm{V}} H i_0 \exp\{\eta_{\mathrm{total}}/b\}, \tag{8.11}$$

for a fully utilized electrode (Bisang *et al.* 1994). The slope of the 'Tafel plot' of such an electrode doubles compared to flat electrodes and the Tafel line is shifted to lower currents according to the changed pre-exponential factor. By proper choice of the values of ρ_{el} and ρ_{ion} the morphology of the electrode matrix, e.g. its porosity, the electrical contact between electrode particles and the turtuosity of the electrolyte pores are accounted for. The higher Φ_Ω, the lower the electrode utilization. For virtually exclusively ohmic polarization the utilization of the electrode is given by

$$(\text{cat. utiliz.})_\Omega \approx \mathrm{f_H}\, \Phi_\Omega^{-1} \tanh \Phi_\Omega. \tag{8.12}$$

(*e*) *Combined concentration polarization and potential drop*

In general, the differential equations (8.1) and (8.8) can be solved simultaneously only by numerical methods. It is, however, possible to also define for this case an adimensional quantity

$$\Phi_{\mathrm{Th}+\Omega} = H(i_0 A_{\mathrm{V}} (\rho_{\mathrm{ion}} + \rho_{\mathrm{el}}) \alpha (1 + \Psi) / 2\Psi b)^{1/2} \exp\{\alpha\eta/2b\}, \tag{8.13}$$

with $\Psi = \nu_{\mathrm{e}} (\rho_{\mathrm{ion}} + \rho_{\mathrm{el}}) \alpha F D c_0 / b$, which characterizes the utilization of the catalyst. The quantity $\Phi_{\mathrm{diff}+\Omega}$ has the limiting values Φ_Ω for $\Psi > 5$ and Φ_{Th} for $\Psi < 0.2$.

(*f*) *Water transport through proton exchange membranes—a dominant factor for PEMFC performance*

The transfer of solvating water molecules by drag of the migrating protons from the anode to the cathode in PEMFs seriously affects the performance of these cells if insufficient supply of water from the moist anode gas at high current densities

leads to a sizeable reduction of the water content of the membrane at the anode side. The reason is a decay of the ionic conductivity of the membrane if the material loses water. Modelling of this effect by Verbrugge and coworkers (Verbrugge & Hill 1988; Verbrugge 1989; Hill & Verbrugge 1990) and by Gottesfeld and coworkers (Springer *et al.* 1994) showed that back diffusion of water from the cathode to anode is most important for mitigating performance losses. It is possible to avoid almost any increase in cell resistance and decrease in cell voltage if the thickness of the Nafion membrane is reduced from 175 to 50 μm.

9. Concluding remarks

The development of materials and production technologies of electrocatalyst, electrodes and cells is far from finished as shown even for PAFCs in a recent paper (Fuller *et al.* 1995). The issue of fuel cell development is today more a matter of material science than of fundamental electrochemical research. In the context of catalyst and electrode morphology optimization modelling of electrode performance is an indispensible tool.

References

Appleby, A. J. & Foulkes, F. R. 1988 Cathode materials: solid oxide electrolyte fuel cells. In *Fuel cell handbook*. pp. 579–611. New York: Van Nostrand.

Aragane, J., Urushibata, H. & Murakashi, T. 1994 Evaluation of an effective platinum metal surface area in a phosphoric oxide fuel cell. *J. Electrochem. Soc.* **149**, 1804–1808.

Bette, J. A. S. 1992 Oxygen electrocatalysis in phosphoric acid fuel cells. In *Proc. Symp. Structural effects in Electrocatalysis and oxygen electrochemistry* (ed. D. Sherson, D. Tryk, M. Daroux & X. Xing), vol. PV–92–11, pp. 573–83. Pennington, NJ: Electrochemical Society.

Bisang, J. M., Jüttner, K. & Kreysa, G. 1994 Potential and current distribution in porous electrodes under charge transfer kinetic control. *Electrochim. Acta* **39**, 1297–1302.

Böhme, O., Leidich, F. U., Salge, H. J. & Wendt, H. 1994 Development of materials and production technologies for molten carbonate fuel cells. *Int. J. Hydrogen Energy* **19**, 349–366.

Brown, A. P., Kucera, G. H., Roche, M. F., Chu, D. D. and Judadochea, E. 1992 Performance of alternative cathodes in molten carbonate melts. In *Fuel Cell Seminar* (Tucson 1992), pp. 125–129. Washington, DC: Courtesy Associates.

Collmann, B. E., Marocco, M., Denisowitsch, P., Koval, C. & Anson, S. C. 1979 Potent catalysis of the electroreduction of oxygen to water by dicobalt porhyrin dimers adsorbed on graphite electrodes. *J. Electroanal. Chem.* **101**, 117–122.

Collmann, J. P., Denisowitsch, P., Konai, Y., Marocco, M., Covol, C. & Anson, F. 1980 Electrode catalysis of the four-electron reduction of oxygen to water by dicobalt face-to-face porphyrins. *J. Am. Chem. Soc.* **102**, 6027–6036.

Cutlip, M. B., Yang, S. C. & Stonehart, P. 1991 Simulation and optimization of porous gas-diffusion electrodes used in hydrogen/oxygen phosphoric acid fuel cells II. Development of a detailed anode model. *Electrochim. Acta* **36**, 547.

Doyon, J. P., Gilbert, T. H., Davies, G. & Paetsch, L. 1987 NiO solubility in mixed alkali/alkaline earth carbonates. *J. Electrochem. Soc.* **134**, 3035–3038.

Durant, R. R. Jr, Bencosme, C. R., Collmann, J. P. & Anson, F. 1983 Mechanistic aspects of the catalytic reduction of dioxygen by cofacial metalloporphyrins. *J. Am. Chem. Soc.* **105**, 2710–2718.

El-Anadouli, B. E. & Ateya, B. G. 1991 Significance of effectiveness factor for flooded porous electrodes. In *Modeling of batteries and fuel cells* (ed. R. E. White, M. W. Verbrugge & F. J. Stockel), vol. PV-91–10, pp. 1–13. Pennington, NJ: Electrochemical Society.

Exner, H. E. 1978 Grundlagen der Sintervorgänge, Verlag Gebrüder Bornträger, Berlin, Stuttgart.

PHILOSOPHICAL TRANSACTIONS OF THE ROYAL SOCIETY A MATHEMATICAL, PHYSICAL & ENGINEERING SCIENCES

Fontes, E., Fontes, M. & Simonsson, D. 1995 A heterogeneous model for the MCFC cathode. *Electrochim. Acta* **40**, 1641–1651.

Fuller, T. F., Luczak, F. J. & Wheeler D. J. 1995 Electrocatalyst utilization in phosphoric acid fuel cells. *J. Electrochem. Soc.* **142**, 1752–1757.

Hill, R. & Verbrugge, M. 1990 Ion and solvent transport in ion-exchange membranes. *J. Electrochem. Soc.* **137**, 886–893.

Ito, T., Kato, K., Kamiya, M. & Kirinuki, H. 1988 Advanced electrocatalysts for phosphoric acid fuel cells. In *Program and Abstracts Fuel Cell Seminar* (October 23–26, Long Beach CA), pp. 160–163. Washington, DC: Courtesy Associates.

Itoh, T. & Katoh, K. 1990 N. E. Chemcat Corp. Platinum alloy Electrocatalyst. Eur. Pat. Appl. EP 386 764.

Jalan, V. M. & Landsman 1979 Fuel cell electrode catalysts from noble metal containing alloys. Belg. Pat. 877 413.

Jalan, V. M. Giner Inc. 1985 Cathode alloy electrocatalysts. Eur. Pat. Appl. 165 024.

Kinoshita, K. 1992 Crystallite site effect in electrocatalysis. In *Proc Symp. Structural Effects in Electrocatalysis and Oxygen Electrochemistry* (ed. D. Shirson, D. Tryk, M. Daroux and X. Xing), vol. PV-92-11, pp. 307–323. Pennington, NJ: Electrochemical Society.

Kinoshita, K. & Stonehart, P. 1988 *Modern aspects of electrochemistry* (J. M. O'Bockris & B. F. Conway), vol. 12, pp. 183. New York: Plenum.

Kirchnerova, J., Klvána, D., Hinatsu, J., Xie, S., Forst, V. , Olveira, J., Anataraman, A. & Goledzinovska, M. 1995 New Ni–Co based perovskites as electrocatalysts in alkaline fuel cells. *Proc. 1st Int. Symp. on new materials for fuel cell systems* (July 9–13, Montreal) (ed. O. Savadogo, P. R. Roberge & T. N. Veziroglu), pp. 190–200. Éditions de l'école polytechnique de Montreal.

Kudo, T., Shimada, T., Nagashima, I., Mori, T., Hishino, K. & Fukui, T. 1995 Development of new materials technology for molten carbonate fuel cells. In *Proc. 1st Int. Symp. on new materials for fuel cell systems* (ed. O. Savadogo, P. R. Roberge & T. N. Veziroglu), pp. 425–436. Éditions de l'école polytechnique de Montréal.

Kunz, H. R. 1991 Variability in nickel oxide cathode dissolution in molten carbonate fuel cells. In *Proc. Symp. Modeling of batteries on fuel cells* (ed. R. E. White, M. W. Verbrügge & J. F. Stockel), vol. PV-91-10, p. 175. Pennington, NJ: The Electrochemical Society.

Mc Intyre, J. D. E. & Peck, W. F. Jr 1980 Electrocatalysis by foreign metal adatoms. In *Proc. Symp. Electrode Processes 1979* (ed. S. Bruckenstein, J. D. E. Mc. Intyre, B. Miller, & E., Yeager), vol. PV 80–3, p. 322–349. Princeton, NJ: Electrochemistry Society.

Mund, K. & v. Sturm, F. 1975 Degree of utilization and specific effective surface area of electrocatalysts in porous electrodes. *Electrochim. Acta* **20**, 463–467.

Mund, K., Richter, G. & von Sturm, F. 1977 Titanium containing Raney-nickel catalyst for hydrogen electrodes in alkaline fuel cells. *J. Electrochem. Soc.* **124**, 1–6.

Ota, K., Mitsushima, S., Kato, S., Asano, A., Yoshitake, H. & Kamiys, N. 1992 Solubilites of nickel oxide in molten carbonate. *J. Electrochem Soc.* **139**, 667–671.

Plomp, L. & Huijsmann, J. P. P. 1995 Materials research in high-temperature fuel cell development. In *Proc. 1st Int. Symp. on new materials for fuel cell systems* (July 9–13 1995, Montreal) (ed. O., Savadogo, P. R., Roberge & T. N., Veziroglu), pp. 388–397. Éditions de l'école polytechnique de Montreal.

Rhines, F. N. 1940 A metallographic study of internal oxidation in solid solutions of α-copper. *Trans. AIME* **137**, 246–287.

Ristic, N. M., Jaksic, J. M. & Jacsic, M. M. 1995 Synergetic electrocatalysts for hydrogen electrode reactions in the light of fermi dynamics and structural bonding factors. In *Proc. Int. Symp. on new materials for fuel cells systems* (July 9–13 1995, Montreal) (ed. O. Savadogo, P. R. Roberge & T. N. Veziroglu), pp. 577–604. Éditions de l'ecole polytechnique de Montreal.

Scholta, J. 1993 Experimentelle Untersuchungen zur Material- und Betriebstechnik phosphorsaurer Brennstoffzellen. PhD thesis. Technische Hochschule Darmstadt.

Springer, T. E., Zawodinski, T. A. & Gottesfeld, S. 1994 Modelling water content effects in polymer electrolyte fuel cells. In *Modeling of batteries and fuel cells* (ed. R. E. White, M. W.

PHILOSOPHICAL TRANSACTIONS OF THE ROYAL SOCIETY A MATHEMATICAL, PHYSICAL & ENGINEERING SCIENCES

Verbrugge & F. J. Stockel), vol. PV 91–10, pp. 209–229. Pennington, NJ: Electrochemical Society.

Stonehart, P. 1990 Development of advanced noble metal–alloy electrocatalysts for phosphoric acid fuel cells (PAFC). *Ber. BunsenGes. Phys. Chem.* **94**, 913–921.

Trasatti, S. 1972 Work function, electronegativity, and electrochemical behaviour of metals III. Electrolytic hydrogen evolution in acid solutions. *J. Electroanal. Chem.* **39**, 163–184.

Tryk, D. A., Zhang, Z., Aldred, W. A., Kim, S., Sherson, D. A. & Yeager, E. 1994 Nickel–platinum bronzes as electrocatalysts for oxygen reduction in acid electrolytes. *Ext. Abstr.* 94–1, abstract 621, pp. 987–988. Pennington, NJ: Electrochemical Society.

Verbrugge, M. 1989 Methanol diffusion in perfluorinated ion-exchange membranes. *J. Electrochem. Soc.* **136**, 417–423.

Verbrugge, M. & Hill, R. 1988 Experimental and theoretical investigation of perfluosulfonic acid membranes equilibrated with aqueous sulfuric acid solutions. *J. Phys. Chem.* **92**, 6778–6783.

Wendt, H. 1988 Commercially available materials for electrolyser construction. In *Electrochemical reactors* (ed. M. I. Ismail), pp. 248–274. Amsterdam: Elsevier.

Yang, S. C., Cutlip, M. B. & Stonehart, P. 1990 Simulation and optimization of porous gas-diffusion electrodes used in hydrogen/oxygen phosphoric acid fuel cells I. Application of cathode model simulation and optimization to PAFC cathode development. *Electrochim. Acta* **35**, 869–878.

Discussion

K. Kendall (*Keele University, UK*). Professor Wendt said that fuel cells, except for direct methanol, always use hydrogen. This is not so. The SOFC uses CO as fuel by direct oxidation, and also CH_4 can be directly oxidized on cerium oxide anodes (paper from Risø labs in 1992).

H. Wendt. Yes, but CO and CH_4 oxidations are much slower processes than H_2-oxidation. Further, vapour has to be added to CH_4 to avoid cracking. Under these conditions CH_4 is steam reformed *in situ* and H_2 becomes the fuel instead of CH_4.

PHILOSOPHICAL TRANSACTIONS OF THE ROYAL SOCIETY A MATHEMATICAL, PHYSICAL & ENGINEERING SCIENCES

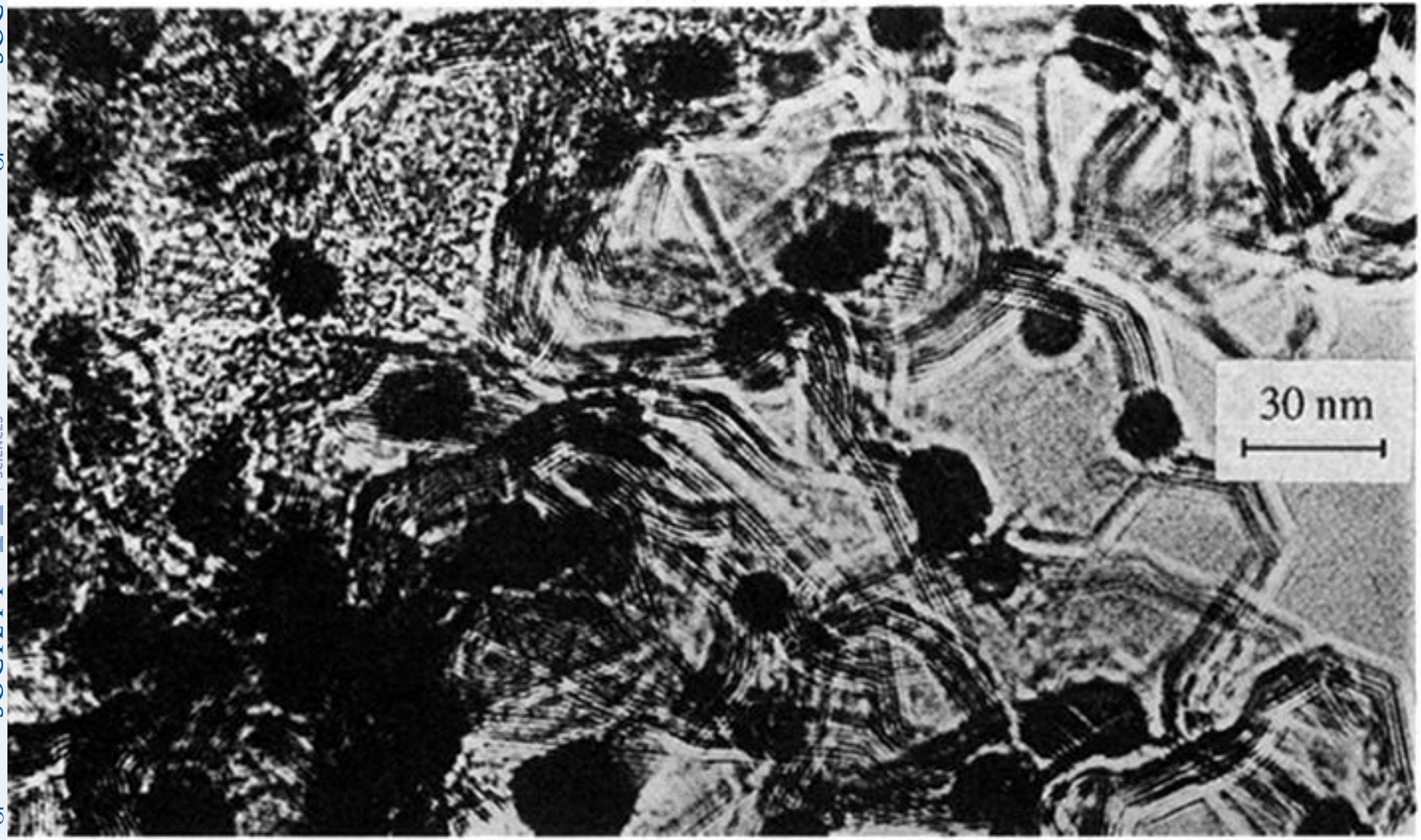

igure 1. Transmission electron micrograph of Pt-activated carbon.

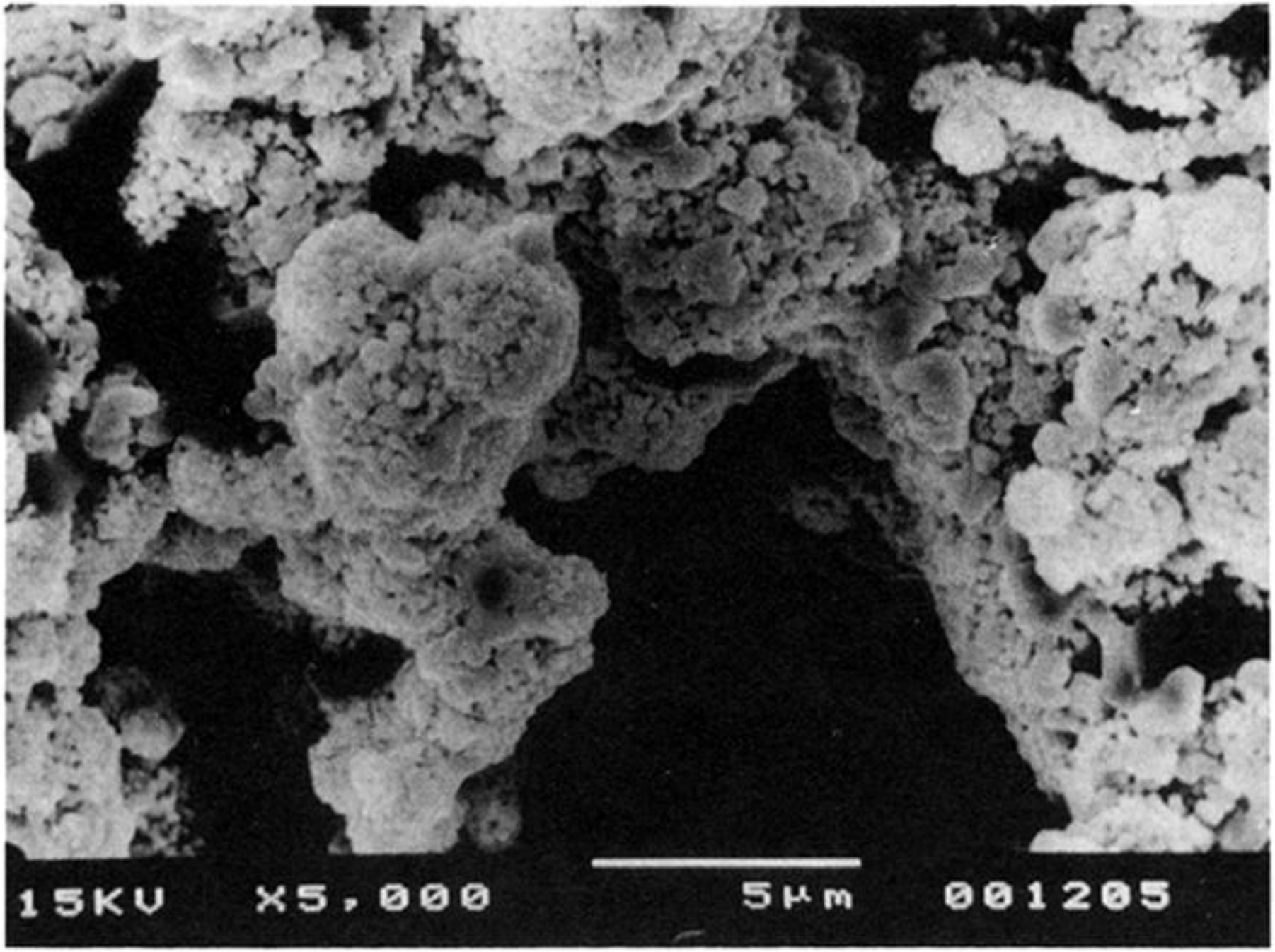

igure 2. Scanning electron micrograph of a NiO cathode for MCFC.

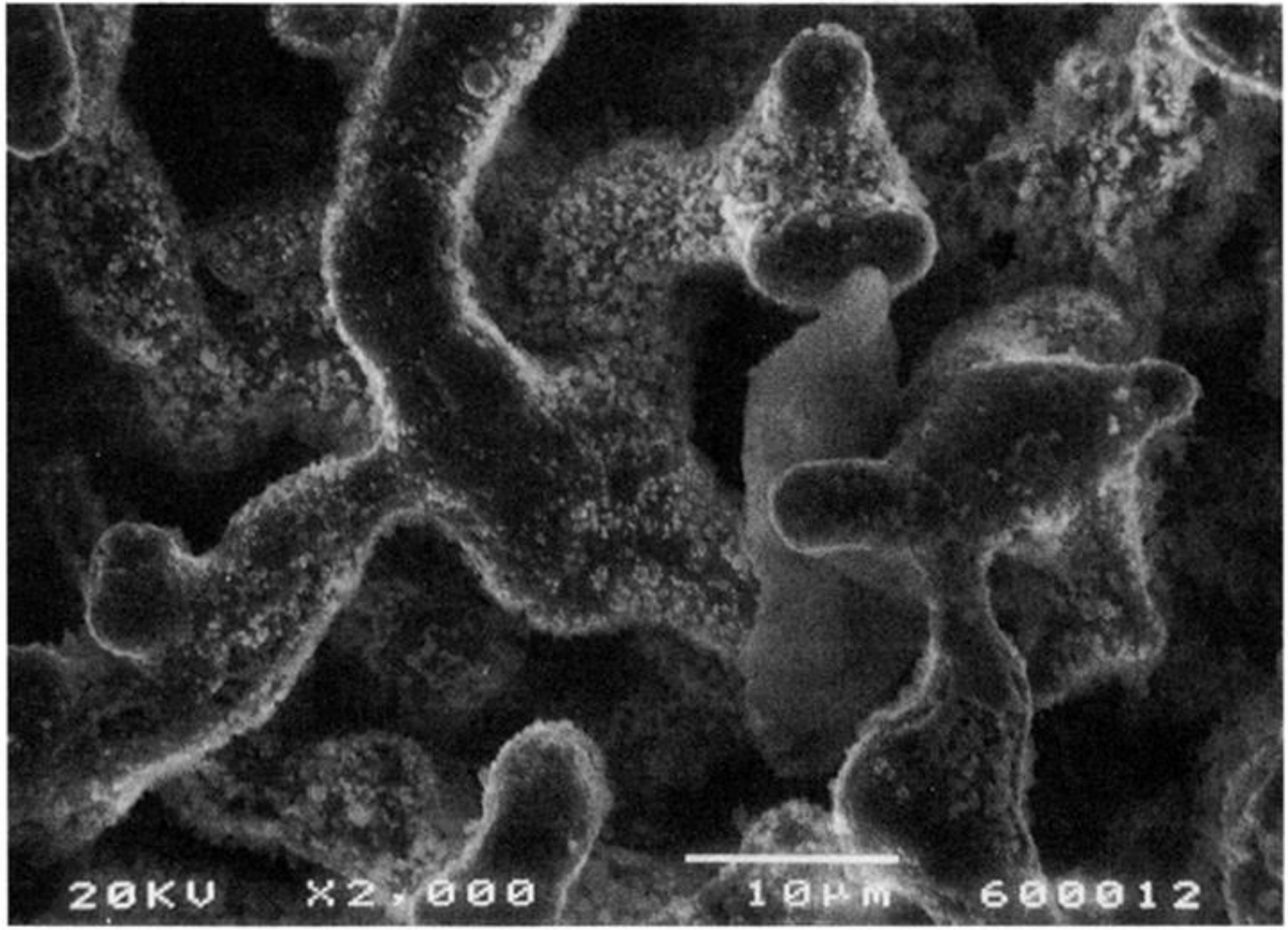

gure 4. Scanning electrode micrograph of Li_2TiO_3-stabilized sintered nickel anode (MCFC).